THE LINEAR ELASTIC DYNAMIC ANALYSIS OF SHELLS OF REVOLUTION BY THE MATRIX DISPLACEMENT METHOD

Stanley Klein*
Richard J. Sylvester*

Aerospace Corporation
San Bernardino Operations
San Bernardino, California

The paper describes the matrix displacement finite element approach to the linear elastic dynamic analysis of shells of revolution under axisymmetric and asymmetric loads. The shell is idealized as a series of conical frusta, joined at nodal circles. The derivation of the mass and stiffness matrices for a shell structure is outlined. A method for solution of the equations of motion is described for this particular type of problem, with special emphasis on the computational aspects of the solution. An especially appropriate finite difference technique is used along with a method for efficiently utilizing the digital computer memory to store and solve a large system of linear simultaneous equations. The solution for a shallow spherical cap under time varying axisymmetric pressure load indicates the scope, speed, and accuracy of the solution method.

SYMBOLS

$A_{\alpha,\beta}$	Integrals defined in the Appendix
$\mathbf{A}(s,\theta)$	Matrix of coefficients introduced in Equation 4
$\mathbf{A}_i$, $\mathbf{B}_i$	Square matrices introduced in Equation 18
$\mathbf{B}$	Matrix of coefficients introduced in Equation 6
C^i	Damping matrix for a structure
$\mathbf{E}^*$	Matrix relating stresses to strains, introduced in Equation 7
$\mathbf{F}(t)$	Column vector of forces as functions of time
$\mathbf{G}$	Square matrix defined in Equation 18
$\mathbf{K}$	Stiffness matrix for a structure
$\mathbf{L}$	Matrix defined in Equation 7
$\mathbf{L}_T$	Lower triangular matrix factor of $\mathbf{G}$, in Equation 20
$\mathbf{M}$	Mass matrix for a structure

*Members of the Technical Staff

SYMBOLS (Cont'd)

$M_s, M\theta, M_s\theta$	Stress couples of a shell
$N_s, N\theta, N_s\theta$	Stress resultants of a shell
N, P, R, S	Square matrices in recurrence relation, Equations 16, and 17
P	Matrix defined in Equation 11
$Q_s, Q\theta$	Meridional shear stress resultants of a shell
$Q, \bar{Q}$	Generalized forces; Fourier cosine and sine coefficients
T	Kinetic energy of element for assumed displacement field
$T_p\ (\theta)$	Applied load per unit length at node p
U	Strain energy of element for assumed displacement field
V	Matrix of coefficients introduced in Equation 10
W	Mechanical work
$\{d(s,\theta,t)\}$	Arbitrary displacement vector introduced in Equation 4
f	Column vector of applied generalized forces and reactions
h	Shell thickness
i	Superscript denoting harmonic number
j	Subscript denoting generalized coordinate number
k	Stiffness matrix for an element
ℓ	Meridional length of the conical element
$[m]$	Mass matrix for an element
n	Subscript denoting time interval
p	Subscript denoting node number
$q_j, \bar{q}_j$	Generalized displacements; Fourier cosine and sine coefficients
$\{q^i\}, \{\dot{q}^i\}, \{\ddot{q}^i\}$	Column vectors of generalized displacements, velocities and accelerations for harmonic number i
r	Radial coordinate
s	Meridional coordinate
t	Time

SYMBOLS (Cont'd)

u, v, w	Axial, circumferential, radial displacement
$\dot{u}, \dot{v}, \dot{w}$	Meridional, circumferential, normal velocity
z	Axial coordinate
$\alpha(t)$	Unknown coefficients as functions of time, Equation 4
$\dot{\alpha}_j^i$	Unknown coefficients for harmonic number i in Equation 8
β	Rotation of meridian and generalized acceleration parameter
θ	Circumferential angle, coordinate
ρ_A	Mass density (mass per unit area) of shell element
ϕ	Angle between meridian and axis (semi-apex angle of cone)
$[\psi]$	Coordinate transformation matrix (introduced in Equation 6)

INTRODUCTION

For an arbitrary shell of revolution, the response to dynamic loadings can be determined by representing the deformation of the shell structure by a finite number of generalized displacements and solving the corresponding equations of motion, viz.,

$$\mathbf{M}^i \ddot{\mathbf{q}}^i(t) + \mathbf{C}^i \dot{\mathbf{q}}^i(t) + \mathbf{K}^i \mathbf{q}^i(t) = \mathbf{F}^i(t) \qquad (1)$$

The square symmetric matrices, $\mathbf{M}^i$ and $\mathbf{K}^i$, are the mass and stiffness matrices of the structure. The column vector, $\mathbf{F}^i(t)$, represents the applied generalized forces and reactions. The column vectors $\mathbf{q}^i(t)$, $\dot{\mathbf{q}}^i(t)$, and $\ddot{\mathbf{q}}^i(t)$ are the generalized displacements, velocities, and accelerations. The square matrix, $\mathbf{C}^i$, is a damping matrix and although the theoretical development that follows includes provisions for this matrix, the actual numerical solutions presented are for undamped structures.

A finite element idealization of the structure with completely arbitrary element size is used. The continuous system is represented by a finite number of degrees of freedom in a physically meaningful way with the matrix displacement method used to calculate an approximation to the stiffness matrix, $\mathbf{K}^i$, directly. Consistent with the approximations involved in using the matrix displacement method, an approximation to the mass matrix, $\mathbf{M}^i$, is generated.

Embodied in the mass and stiffness representation of the shell structure, a shell analysis, which permits arbitrary meridional shapes, thickness and material property variation in the meridional direction, varying meridional mass distribution, and stiffening of arbitrary portions of the shell, is presented. Axisymmetric and asymmetric distributed and line loading conditions can be represented in the vector, $\mathbf{F}^i(t)$, and various boundary conditions may be used in the solution of Equation 1. In its present form, the analysis is limited to homogeneous isotropic single layer (or equivalent multilayer) shells under the assumptions of thin shell theory.

The analysis presented is comprised of two parts: (1) the finite element shell analysis consisting of the derivation of $\mathbf{M}^i$ and $\mathbf{K}^i$ with a discussion of their accuracy and limitations; and

(2) the mathematical solution of Equation 1 with a brief discussion of the features of a digital computer program written for this solution.

In view of the publication of a number of documents detailing the theoretical background of the finite element shell analysis (References 1, 2, and 3) and the associated computer codes (References 4 and 5), which output $\mathbf{M}^i$ and $\mathbf{K}^i$ for use in Equation 1, only a brief description of this analysis is given for continuity of presentation. The many solutions for the static analysis of shells (References 3 and 6) give a good indication of the accuracy of $\mathbf{K}^i$, while the accuracy of $\mathbf{M}^i$ will be discussed here. An elaborate discussion of the development of the finite element technique, the problem areas, scope, limitations, and associated computer codes has also been given (Reference 6).

Thus, a large portion of this work is devoted to the mathematics involved in the dynamic solution, with special attention to the computational aspects of the solution.

Idealization of the Structure and Loading

The complete shell is idealized into a series of conical frusta joining nodal circles which lie in the shell surface (Figure 1). A right-handed system of cylindrical coordinates is used in the analysis, viz., axial distance z, circumferential angle θ, and radial distance r. The behavior of the shell is characterized by a set of generalized displacements of a nodal circle at station z. These generalized displacements, $\mathbf{q}^{i*}$, are the Fourier coefficients of u, v, w, and β expanded in a Fourier series in θ, where u, v, and w are the axial, circumferential, and radial displacements of a point of the circle, and β is the rotation at the point in a plane containing the axis of the shell and the meridian in the shell surface which passes through the point. The superscript i on $\mathbf{q}^i$ is called the harmonic number.

The corresponding generalized forces may be visualized as representing line loads applied at the nodes and written as

$$\pi r_p T_p(\theta) = \frac{1}{2} Q_p^0 + \sum_{i=1}^{m} Q_p^i \cos i\theta + \sum_{i=1}^{m} \bar{Q}_p^i \sin i\theta \qquad (2)$$

where Q_p^i and $\bar{Q}_p^i$ are the generalized forces corresponding to q_p^i and $\bar{q}_p^i$ respectively, r_p is the radius of the p^{th} nodal circle and T_p is an applied load per unit length in a representative direction.

The displacements u, v, and w are positive in the positive directions of z, ϑ, and r and β is positive if it corresponds to a positive value of $\partial w/\partial z$ along the meridian. The force per unit length, T_p, is positive if it does positive work when displaced through a positive value of q_p.

It may be observed that the generalized forces have been defined so that the total work done by the forces in an incremental displacement (du, dv, dw, $d\beta$) is,

$$dW = \sum_j \left\{ Q_j^0 \, dq_j^0 + \sum_{i=1}^{m} Q_j^i \, dq_j^i + \sum_{i=1}^{m} \bar{Q}_j^i \, d\bar{q}_j^i \right\} \qquad (3)$$

where the subscript j denotes the generalized coordinate number.

The generalized displacements may be regarded as the independent variables in terms of which the analysis is carried out. If there are n nodes and the highest harmonic number used is m, the system may be said to have $4n(2m+1)$ degrees of freedom.

*The time dependence of the generalized displacements, generalized forces, and related quantities will be understood from this point on.

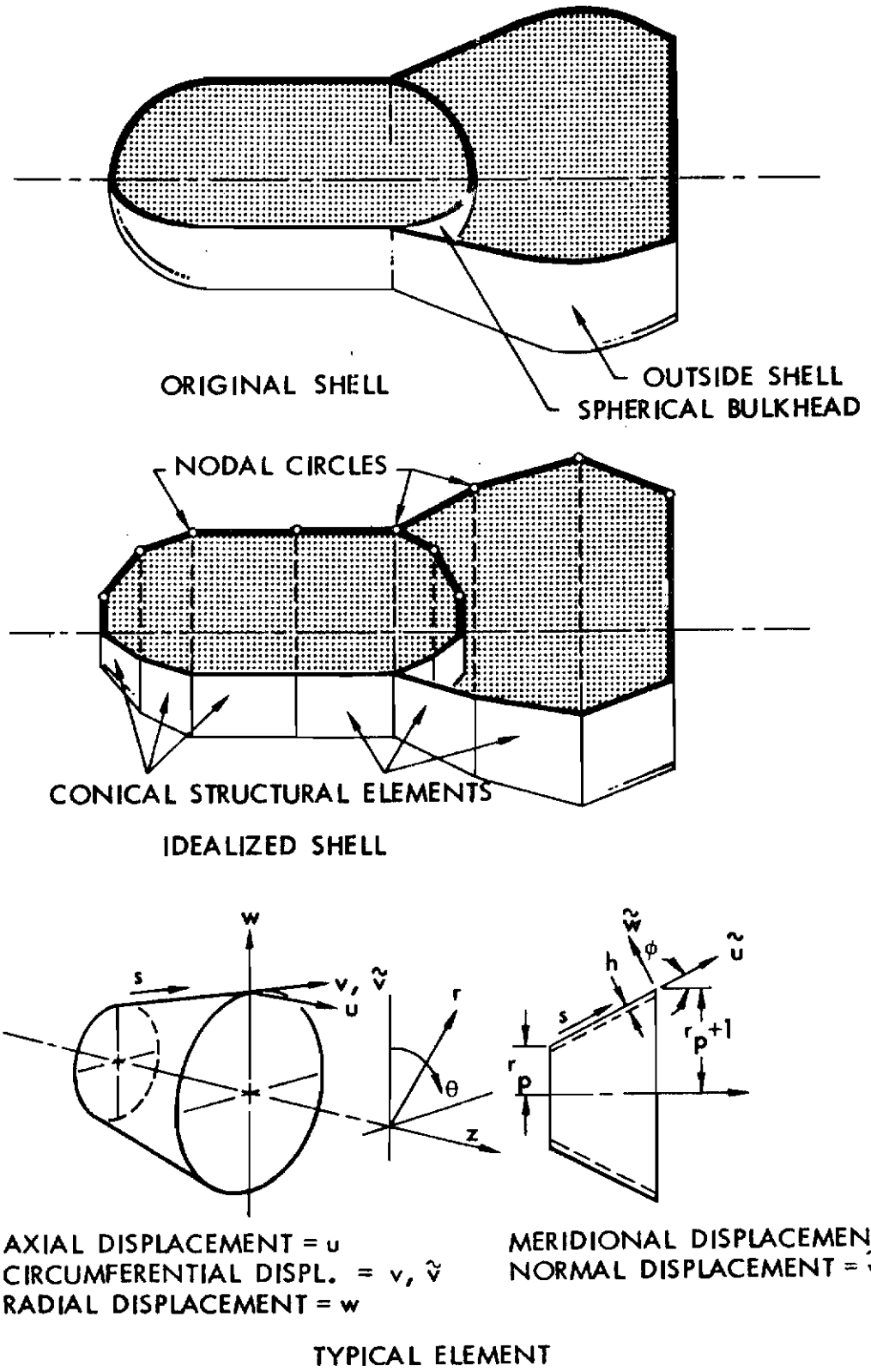

Figure 1. Diagrams to Illustrate the Idealization of a Shell of Revolution for Analysis

The elastic behavior of the shell element (i.e., the conical frustum) is sufficiently described if the linear relationship between the generalized forces and the generalized displacements of the two adjacent nodal circles can be written. This relationship defines the element stiffness matrix, $[k]$, which is an (N x N) square matrix, where N = 16m+8 characterizing a 2 node system with m being the highest harmonic. The shell equations for the conical element uncouple in harmonics (Reference 1) so that k may be partitioned into (8 x 8) squares, k^i, representing the various harmonics with all off-diagonal partitions null.

Assuming the element stiffness matrix is known, a structural stiffness matrix, K, may be obtained by superposing the element stiffnesses, k. This is done according to the equilibrium equation in each direction at each node, which equates the applied force to the sum of the forces acting on the elements bounded by the node (Reference 1, Section 3.3). Furthermore, since k uncouples in harmonics, so does K, resulting in a 4n x 4n symmetric matrix, K^i, for each harmonic.

In a similar manner, the structural mass matrix for each harmonic, M^i, is obtained by superposition of the element mass matrices, m^i, (Reference 1).

THE ELEMENT STIFFNESS AND MASS MATRICES

It is obvious from the above discussion that the key step in the analysis is the derivation of k^i and m^i. The use of the matrix displacement method to derive an approximation to the element (in this case a conical frustum) stiffness matrix is a well known procedure (Reference 1). In general, it consists of first assuming a displacement field for the element, such as

$$d^i(s, \theta, t) = A^i(s, \theta)\ a^i(t) . \tag{4}$$

Then after substituting the strain-displacement relations, written in terms of $a^i(t)$, and the stress-strain relations into the strain energy, U^i, of a linear elastic element deforming in the assumed manner, a simple comparison with the general matrix equation for U^i, i.e.,

$$U^i = \frac{1}{2}\ q^i\ k^i\ q^i \tag{5}$$

leads to the desired result. For the conical element this is

$$k^i = \psi\ (B^{-1})^T\ L^i\ B^{-1}\ \psi^T \tag{6}$$

where ψ is a coordinate transformation matrix relating shell coordinates to system coordinates, B is evaluated by substituting the nodal values of s in Equation 4, and L^i is defined as

$$\underset{8x8}{L^i} = \int_A (W^i)^T\ E^*\ W^i\ dA \tag{7}$$

The W^i matrix relates the strains to the displacement parameters, $a^i(t)$, and E^* is a matrix of coefficients in the stress-strain relations. Further details including the explicit form of the above matrices are available (Reference 6).

An approximation to the element mass matrix, a symmetric matrix of coefficients relating the generalized forces and generalized accelerations of the bounding nodes, may be obtained by using the exact same displacement function given in Equation 4. As such it is consistent with

the element stiffness matrix (Reference 7). Remembering that the displacements are functions of time, the assumed displacement field may be differentiated with respect to time to give a velocity field and may be written explicitly for the conical element as follows:

$$\dot{\tilde{u}}^i = (\dot{\alpha}_5^i + \dot{\alpha}_6^i\, s)\cos i\theta$$

$$\dot{\tilde{v}}^i = (\dot{\alpha}_7^i + \dot{\alpha}_8^i\, s)\sin i\theta \tag{8}$$

$$\dot{\tilde{w}}^i = (\dot{\alpha}_1^i + \dot{\alpha}_2^i\, s + \dot{\alpha}_3^i\, s^2 + \dot{\alpha}_4^i\, s^3)\cos i\theta$$

Displacement components $\tilde{u}^i, \tilde{v}^i, \tilde{w}^i$ correspond to shell coordinates (see Figure 1).

The kinetic energy of translation for an element deforming in this manner is

$$T^i = \frac{1}{2}\rho_A \int_A \left[(\dot{\tilde{u}}^i)^2 + (\dot{\tilde{v}}^i)^2 + (\dot{\tilde{w}}^i)^2\right] dA \tag{9}$$

where ρ_A is the mass per unit surface area (mass density) and is constant for each element. By writing

$$\int_0^{2\pi} \left[(\dot{\tilde{u}})^2 + (\dot{\tilde{v}})^2 + (\dot{\tilde{w}})^2\right] r\, d\theta = \pi\, (\dot{\alpha}^i)^T\, \mathbf{V}\, \dot{\alpha}^i\,, \tag{10}$$

substituting this result into Equation 9 and defining

$$\mathbf{P} = \int_0^{\ell} \mathbf{V}\, ds \tag{11}$$

the expression for the kinetic energy becomes

$$T^i = \frac{\pi\rho_A}{2}\, (\dot{\alpha}^i)^T\, \mathbf{P}\, \dot{\alpha}^i \tag{12}$$

The relationship of the coefficients $\dot{\alpha}^i$ to the generalized velocities $\dot{q}^i$ is

$$\dot{q}^i = \boldsymbol{\psi}\, \mathbf{B}\, \dot{\alpha}^i \tag{13}$$

where $\mathbf{B}$ and $\boldsymbol{\psi}$ have the same meaning as in Equation 6.

Solving for $\dot{\alpha}^i$ in terms of $\dot{q}^i$, substituting the result into Equation 12, and comparing with the general matrix equation for the kinetic energy of a linear elastic element, i.e.,

$$T^i = \frac{1}{2}\, (\dot{q}^i)^T\, \mathbf{m}^i\, \dot{q}^i \tag{14}$$

it is seen that

$$\mathbf{m}^i = \pi\rho_A\, \boldsymbol{\psi}\, (\mathbf{B}^{-1})^T\, \mathbf{P}\, \mathbf{B}^{-1}\, \boldsymbol{\psi}^T \tag{15}$$

The expression $\pi\rho_A \left(\mathbf{B}^{-1}\right)^T \mathbf{P}\, \mathbf{B}^{-1}$ is the mass matrix, $\tilde{\mathbf{m}}^i$, referred to shell coordinates. The integrals required in $\mathbf{P}$ are also required in $\mathbf{L}^i$, which aids the computation. Unlike $\mathbf{L}^i$ however, $\mathbf{P}$ is independent of i for $i \geq 1$, and its form for $i = 0$ is obtained simply by multiplying each coefficient in $\mathbf{P}$ by 2.

Accordingly, the mass matrix is calculated only once; this value serves for all harmonics. The **V** and **P** matrices are listed in the Appendix.

MATHEMATICAL ANALYSIS OF THE EQUATIONS OF MOTION

The element stiffness and mass matrices (Equations 6 and 15), their use in constructing the mass and stiffness matrices of a structure, **M** and **K**, and the solution of shells under static loads have been programmed in FORTRAN for an IBM 7094 (References 4, 5). In addition, these computer codes, called SABOR I (axisymmetric response) and SABOR III (asymmetric response) output **M** and **K** on tape for use in the solution of Equation 1.

Considering that to obtain an accurate solution for a complex shell structure under sharply varying loads may require 100 elements, and remembering there are four generalized displacements (degrees of freedom) at each node, the system of linear second order differential equations represented in Equation 1 will consist of 400 or so simultaneous equations in 400 unknowns. With this in mind, for immediate application any solution proposed must be specifically oriented for use with the digital computers presently available.

The classical limitations of high speed digital computers are three in number: (1) computational accuracy, (2) length of computational time (economy of the solution), and (3) memory size or storage capacity. Even with the present generation of computers, these limitations remain imposing for the system of equations under discussion.

In brief, and within the framework of the FORTRAN IV programming language, these three limitations are met as follows: (1) double precision arithmetic is mandatory in order to retain computational accuracy, (2) a method of numerical integration with a high degree of stability must be used in order that the time necessary for the integration and the corresponding computer expense be reduced, and (3) in order to incorporate a large system of equations within the memory of a computer, it is important to take advantage of the unique characteristics of the problem formulation and store only the necessary information. The details of how the latter two principles are implemented are given below.

FINITE DIFFERENCE SOLUTION

The governing criterion for a method of numerical integration of a large system of differential equations is numerical stability. For this stability property, most methods of integration of the second order differential equations of motion require an interval of integration which is a fraction of the shortest natural period of vibration of the structure. For large systems of equations the shortest natural period may be extremely small, resulting in many hours of computational time, using a digital computer for the integration.

A notable exception to this stability rule is the method of computation presented by Chan, Cox, and Benfield (Reference 8). For the generalized acceleration parameter, $\beta = 1/4$, any interval of integration is stable, and as a result, this finite difference scheme was chosen. A discussion of the β parameter and its effect on the stability of the numerical integration is given in the above reference.

The recurrence relation resulting from the finite difference formulation of Equation 1 is:

$$\mathbf{N}\,\mathbf{q}_{n+1} = \mathbf{P}\,\mathbf{q}_{n} - \mathbf{R}\,\mathbf{q}_{n-1} + \frac{h^2}{4}\left(\mathbf{f}_{n+1} + 2\mathbf{f}_{n} + \mathbf{f}_{n-1}\right) \tag{16}$$

where

$$N = M + \frac{h}{2} C + \frac{h^2}{4} K$$

$$P = 2\left(M - \frac{h^2}{4} K\right)$$

$$R = M - \frac{h}{2} C + \frac{h^2}{4} K .$$

N, **P**, **R**, **M**, **C** and **K** are square matrices (the latter three given in Equation 1), **q** is a column matrix, **f** is a column matrix denoting applied generalized forces and reactions (same as **F** in Equation 1), and n denotes the time interval under consideration.

The given information for a dynamic problem is usually in the form of an initial displacement vector, $\mathbf{q}_0$, an initial velocity vector, $\dot{\mathbf{q}}_0$, and a time history of the force distribution starting with an initial force vector, $\mathbf{f}_0$. Since the recurrence relation in Equation 16 gives the displacement vector at any time step in terms of the displacement vectors of two previous time steps, a special starting equation must be used. It is:

$$N q_1 = S q_0 + h M \dot{q}_0 + \frac{h^2}{4} (f_1 + f_0) \tag{17}$$

where

$$S = M + \frac{h}{2} C - \frac{h^2}{4} K$$

The complete derivation of Equations 16 and 17 has been given in the Appendix of the Chan, Cox and Benfield paper (Reference 8).

TRIDIAGONAL FORM

The recurrence relation and starting procedure given in Equations 16 and 17 contain square coefficient matrices of a special form, namely, matrices which may be partitioned into smaller square matrices such that the particular matrix is tridiagonal in terms of its matrix elements. For example,

$$G = \begin{bmatrix} A_1 & B_1 & 0 & 0 & 0 \\ B_1 & A_2 & B_2 & 0 & 0 \\ 0 & B_2 & A_3 & B_3 & 0 \\ 0 & 0 & B_3 & A_4 & B_4 \\ 0 & 0 & 0 & B_4 & A_5 \end{bmatrix} \tag{18}$$

where $\mathbf{A}_i$ and $\mathbf{B}_i$ are square matrices and **N**, **P**, **R**, and **S** have the same form as **G**. The symmetry property of the matrices has been considered. All that need be stored in the computer memory to represent such a matrix is a two-dimensional array, **A** (I, J), and a three-dimensional array, **B** (I, J, K). Any operations involving the **G** matrix are then performed with sophisticated subscript arithmetic. The array called **A** (I, J) utilizes the first subscript to indicate which of the **A** submatrices is involved, and the second subscript to designate which element of that submatrix is involved. Only the upper triangular part of **A** (I, J) is stored as a vector because of the symmetry property. The array called **B** (I, J, K) utilizes the first subscript to indicate which of the **B** submatrices is involved and the second and third subscripts to designate the row and column of the particular element required from that submatrix.

In a recurrence relation, such as Equation 16, it is possible to invert the first coefficient matrix, $\mathbf{N}$, and premultiply the entire relation by this inverse, thus solving for $\mathbf{q}_{n+1}$. In general, however, $\mathbf{N}^{-1}$ will be fully populated. Thus, in order to keep everything in memory, it is necessary to either reduce the order of the system of equations drastically, or to go "on and off" magnetic tape or auxiliary storage. The above alternatives are deemed unsatisfactory since the first limits the utility of the method and the second is very time consuming and expensive.

The approach adopted, in place of inverting $\mathbf{N}$ and storing its inverse, is to solve, at each step of the numerical integration, a linear system of algebraic equations (Equation 16), represented in general by

$$\mathbf{G}\,\mathbf{q}_{n+1} = \mathbf{b}_n \tag{19}$$

where $\mathbf{b}_n$ represents a column vector (e.g., the right hand side of Equation 16).

The form of $\mathbf{G}$ (Equation 18) is particularly suitable for factoring into the product of a lower and upper triangular matrix, one being the transpose of the other. This factoring procedure preserves the zero elements in the original $\mathbf{G}$ matrix and thus introduces no additional storage requirement other than that required for $\mathbf{G}$. In addition, performing the factorization once at the beginning of the computation, produces the set of factors which are used repeatedly during the subsequent solutions of the linear system of equations (Equation 19). The factoring of $\mathbf{G}$ and the solution of Equation 19 outlined below is very similar to Cholesky's method (Reference 9), and as such has the speed, efficiency, and accuracy required for the solution of a large system of linear algebraic equations (e.g., Equation 16).

For this solution, Equation 19 is rewritten in factored form as

$$\mathbf{L}\,\mathbf{L}^T\,\mathbf{q}_{n+1} = \mathbf{b}_n \tag{20}$$

where $\mathbf{L}$ is the lower triangular factor of $\mathbf{G}$ and $\mathbf{L}^T$ is the transpose of $\mathbf{L}$. $\mathbf{L}$ is stored in memory in the same form suggested for $\mathbf{G}$, whereas $\mathbf{L}^T$ is not stored at all. Defining

$$\mathbf{L}^T\,\mathbf{q}_{n+1} = \mathbf{x}_{n+1}, \tag{21}$$

Equation 20 takes the form

$$\mathbf{L}\,\mathbf{x}_{n+1} = \mathbf{b}_n \tag{22}$$

This may be solved very rapidly from top to bottom, for $\mathbf{x}_{n+1}$ by systematic algebraic substitutions, full advantage being taken of the lower triangular form of $\mathbf{L}$. With the vector $\mathbf{x}_{n+1}$ known, Equation 21 is solved for $\mathbf{q}_{n+1}$, taking advantage of the upper triangular form of $\mathbf{L}^T$ and solving from bottom to top.

DYNAMIC ANALYSIS PROGRAM

A computer code, called DRASTIC* (Dynamic Response Analysis of Shells under Time-dependent and Impulse Conditions), has been written in FORTRAN IV using double precision arithmetic. This code solves the linear system of algebraic equations, Equations 16 and 17, at each integration step for a given set of force vectors called from tape. These force vectors are calculated at the beginning of the computation from the given applied force distribution and stored on tape for subsequent use.

*The authors wish to thank Mr. G. Urmston of the Computation and Mathematics Center, Aerospace Corporation, for his efforts on this program.

The program accepts as input the structural mass and stiffness matrices output by the SABOR codes for the free-free structure, and converts them to the form of the G matrix Equation 18. Displacement boundary restraints are handled within DRASTIC. In its present form DRASTIC analyzes only undamped structures and no provisions are made for the C' matrix. Thus, only 2 matrices, **N** and **P**, need be constructed from **M** and **K** (as **N** = **R** and **P**=2**S**) for use in Equations 16 and 17. **M** and **K** are replaced by **N** and **P** in storage, and then **N** is replaced by its lower triangular factor.

For a given integration interval the program provides a solution at each time step as outlined above, and then outputs displacement, velocity, and acceleration vectors at designated equal time intervals. Supplementary calculations, utilizing a stress matrix from the SABOR programs and the above displacement vector output, give a solution for the dynamic stress resultants and stress couples at the same time intervals.

The DRASTIC code has been written in such a way as to efficiently utilize most of the available core storage of the IBM 7094. Approximately 100 finite elements are permitted for each individual harmonic solution. In the next section the speed and accuracy of the calculations will be demonstrated.

RESULTS OF CALCULATIONS

As an example of the type of shell problem that may be solved with the DRASTIC code, consider a shallow spherical cap with a clamped support at one edge. A solution is given for an axisymmetric pressure loading which is uniformly distributed in the meridional direction and varies as a Heaviside step function in time. The sign convention for the shell stress resultants (Figure 2), and the geometry, material properties, and applied force (Figure 3) are presented.

Five curve plots (Figure 4) graphically illustrate the output. These plots are better understood in terms of the step function loading, which is an initial impulse at t=0 followed by a constant pressure independent of time. Without damping the transient solution of a shell under this loading will oscillate about the steady-state solution, the latter being the same as the response to a static pressure load. This is seen to be the case with the transient solution having a period approximately equal to 1.6 msec.

Plots of the axial displacement at the center of the spherical cap (Figure 4a) and at a point between the center and the fixed end (Figure 4b) are presented first. The static response at these points, obtained from SABOR I output for 14-, 27-, and 42-element solutions, is presented on these graphs as horizontal lines. Negligible difference is seen between the three static results when using the scale required for the dynamic response plots. The same negligible difference is seen between the dynamic results for the three different structural models, with these dynamic solutions converging in the same way as the static solutions.

Presented next is a plot of the meridional tension at the fixed end (Figure 4c). The results are similar in nature to the axial displacement curves, and are carried out in a like manner to a final time of three msec. As with the displacement curves the solutions for 14, 27, and 42 elements are plotted as a single curve.

The last set of curves (Figure 4d) give the moments, meridional and circumferential, at the fixed end. The remarks made for the three previous curves apply to the moment plots, which exhibit the same type of periodicity and oscillation about the static response. The lack of "smoothness" in the moment curves is the result of high frequency response in the radial displacement and rotation curves at the fixed end (not shown here), these displacements being important in the computation of the fixed edge moments. Also presented on this graph is the result for the meridional moment, M_s, obtained by an eigenvalue-normal mode solution in a paper by L. R. Koval and P. G. Bhuta (Reference 10). Considering that only transverse inertia

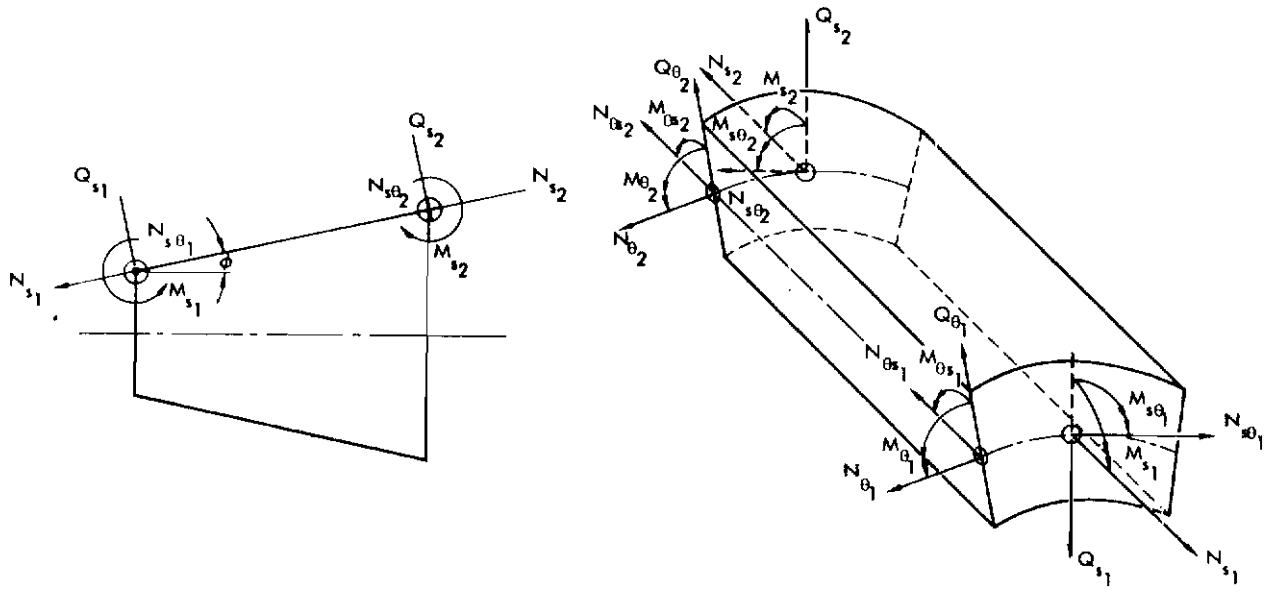

Figure 2. Stress Resultants in Shell Coordinates

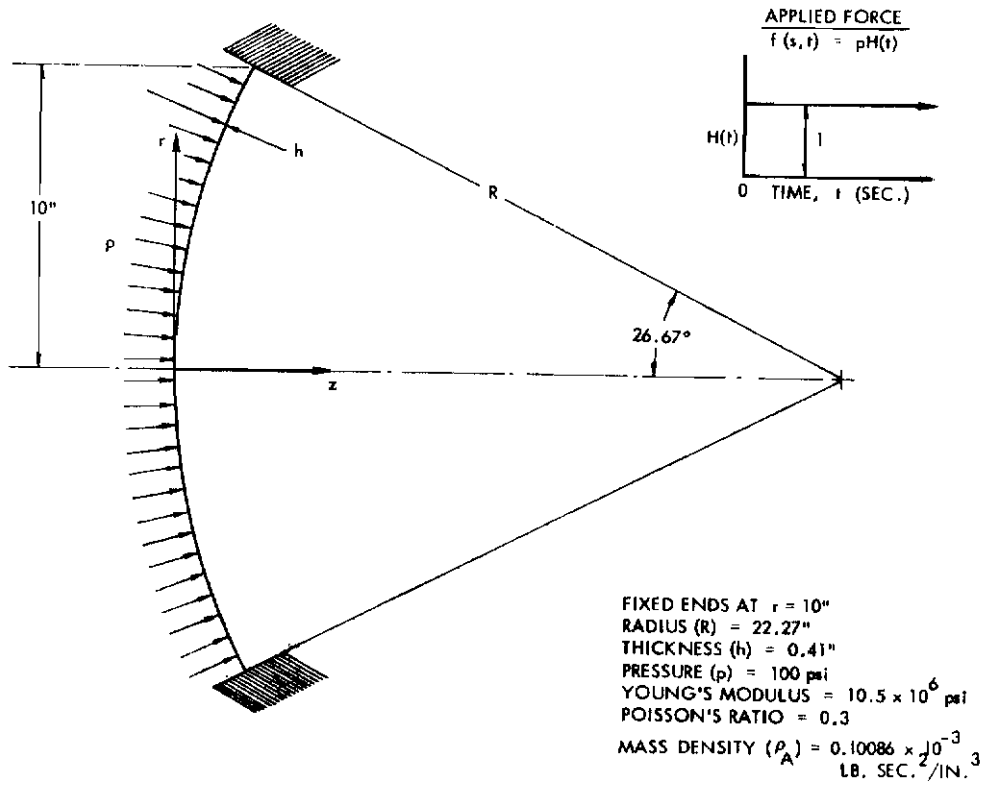

Figure 3. Geometry, Properties, and Applied Force Spherical Cap

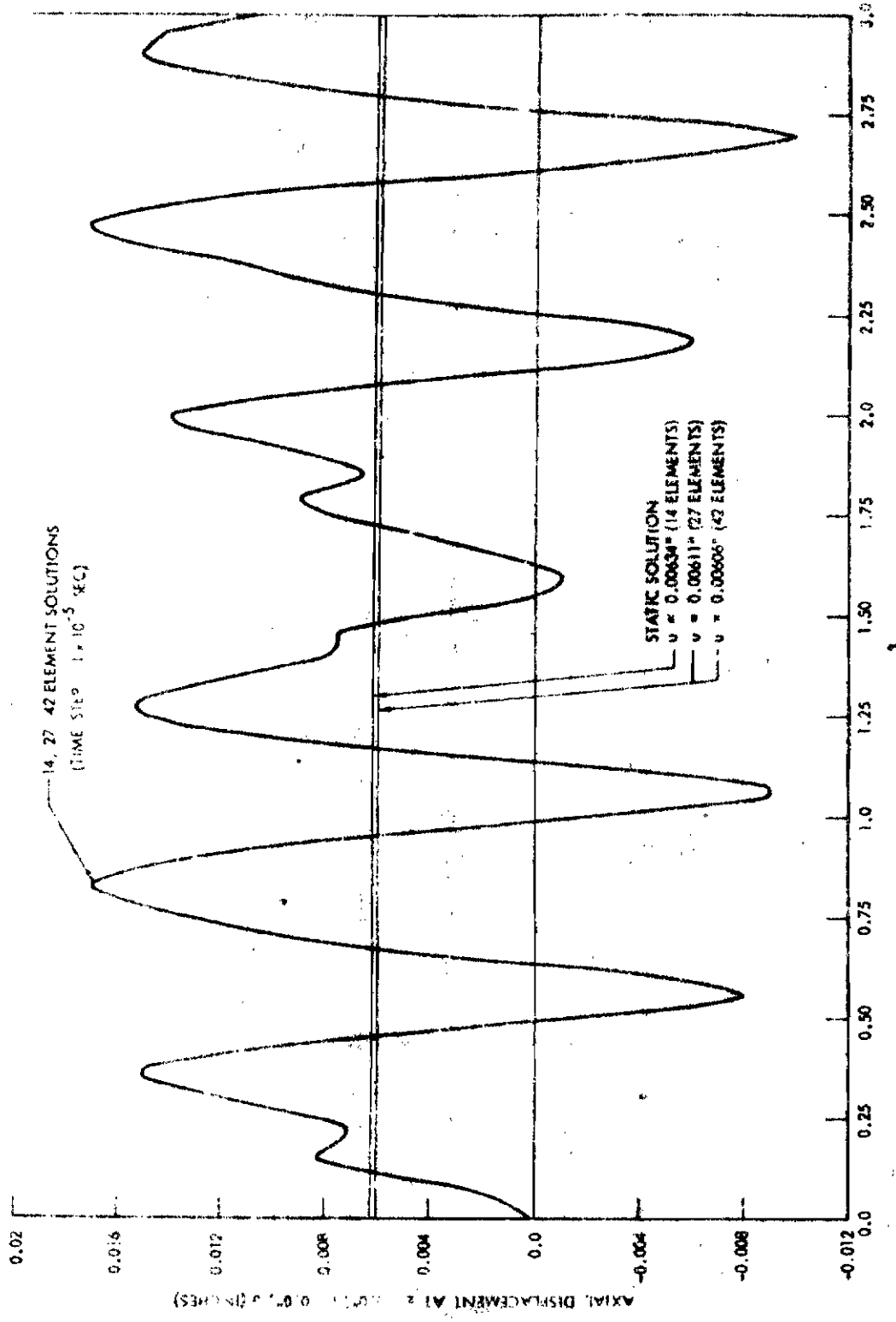

Figure 4a. Shallow Spherical Cap Under Axisymmetric Dynamic Loading

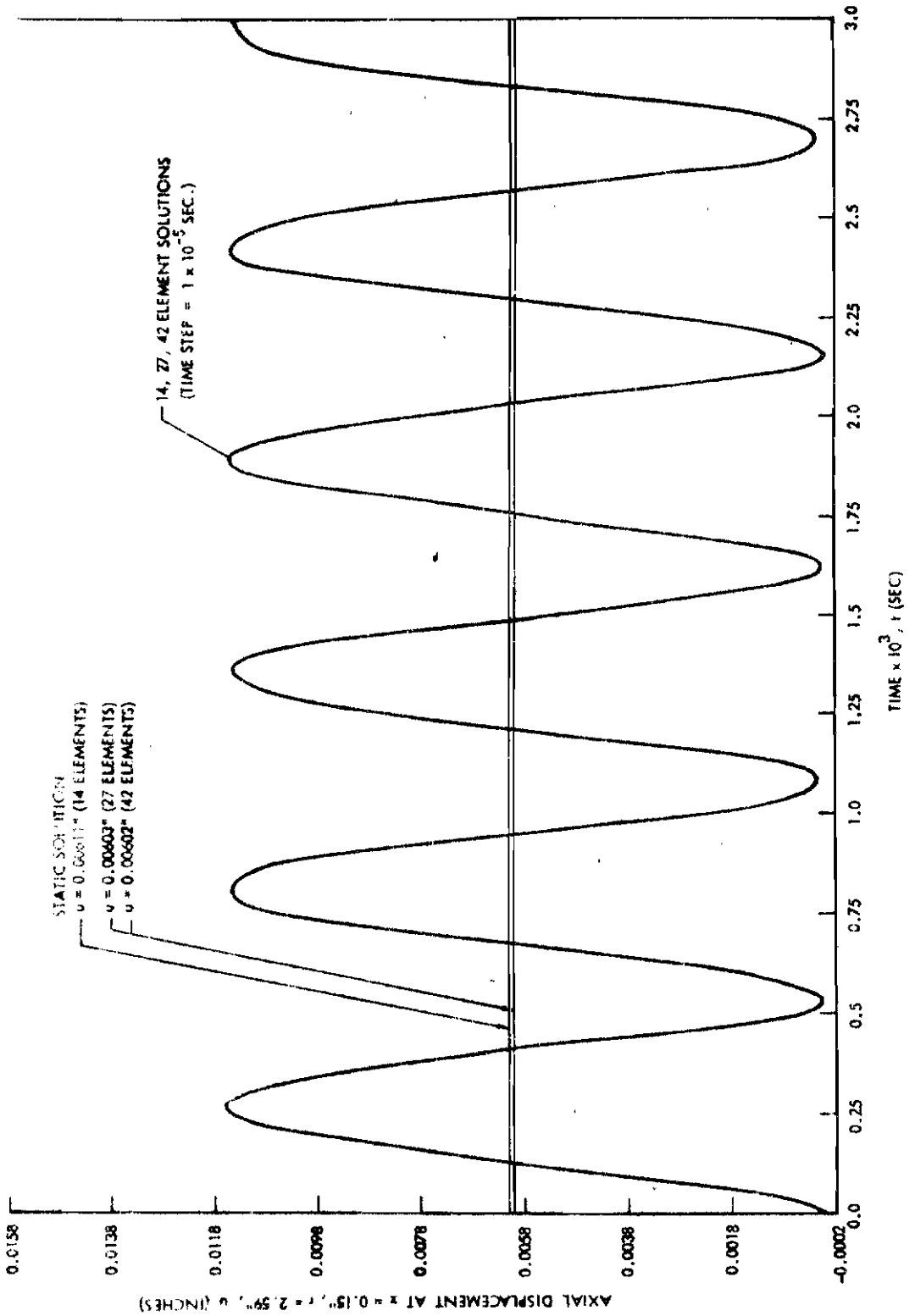

Figure 4b. Shallow Spherical Cap Under Axisymmetric Dynamic Loading

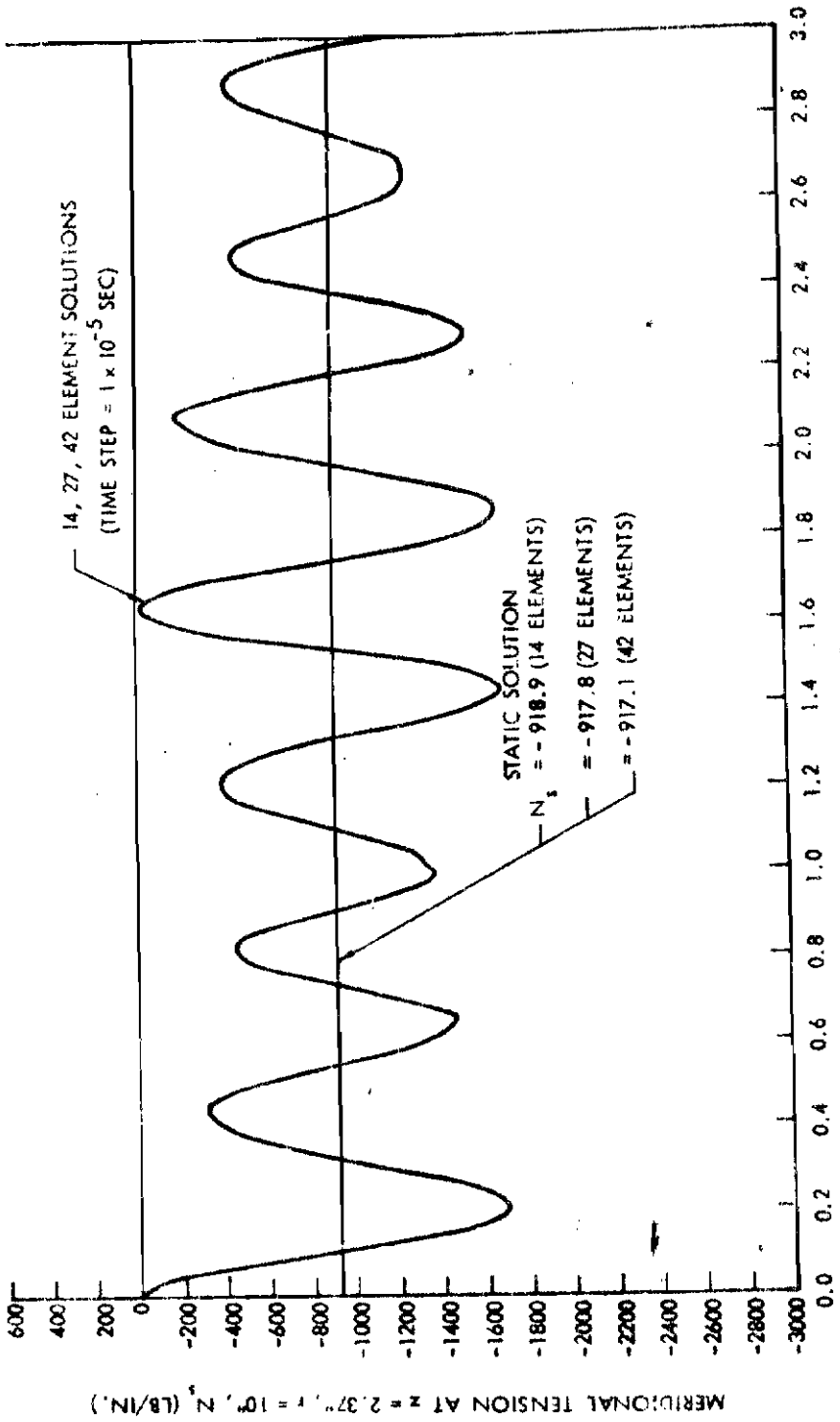

Figure 4c. Shallow Spherical Cap Under Axisymmetric Dynamic Loading

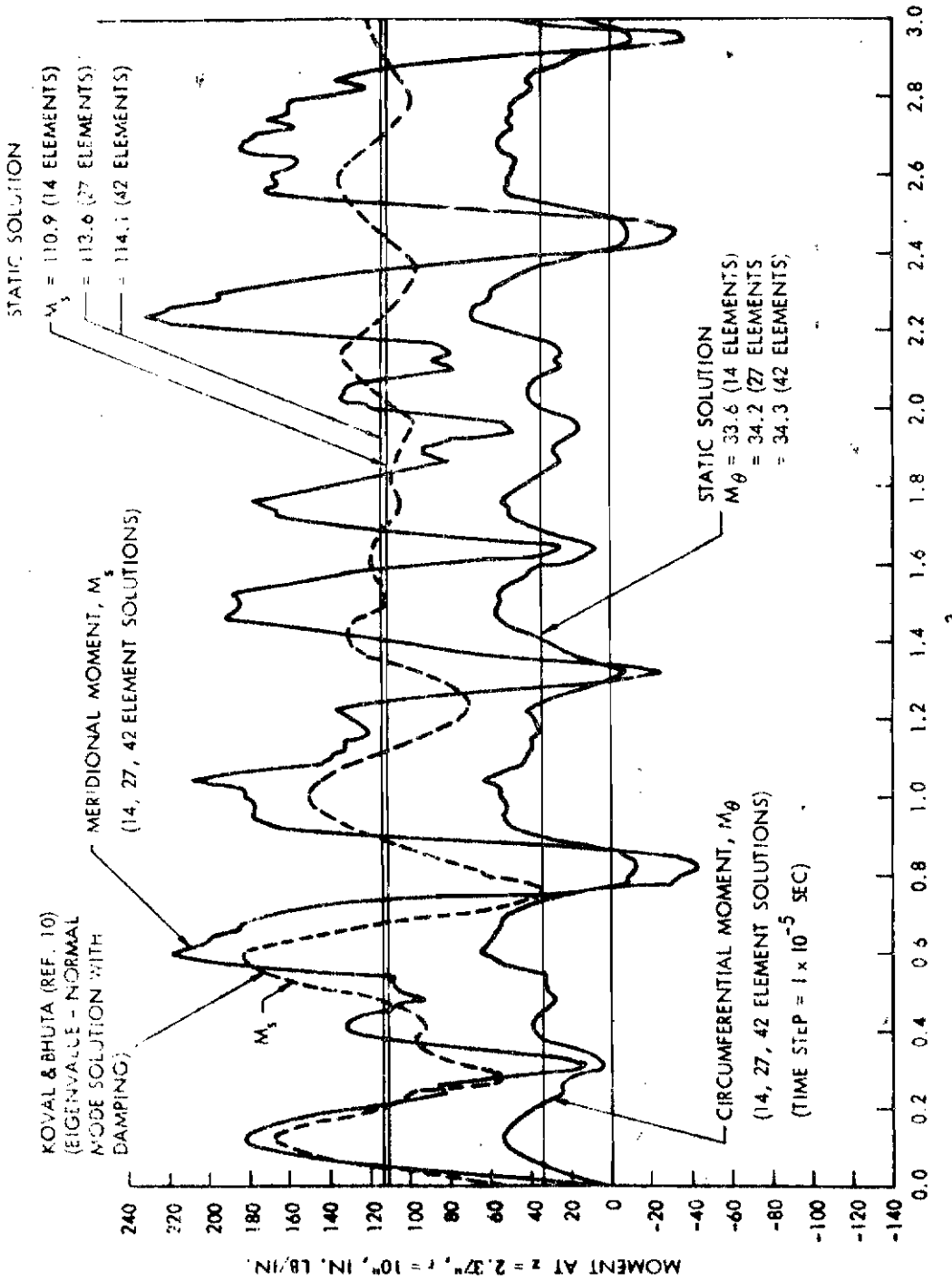

Figure 4d. Shallow Spherical Cap Under Axisymmetric Dynamic Loading

was taken into account in the solution, only 20 modes were used, and that damping was taken at 5 percent of critical for each mode, this solution compares very well with the results from DRASTIC. Whereas the DRASTIC solution oscillates about the static response, the Koval and Bhuta transient solution is almost completely damped out to the static value by the end of three msec.

It is interesting to point out that the 42-element DRASTIC solution of this spherical cap problem consisted of 300 integration steps, the storage of mass and stiffness matrices of rank 129, the solution of 129 simultaneous linear algebraic equations at each integration step, and the output of 150 displacement, velocity, acceleration, and stress (5 values) vectors. The entire procedure was accomplished in 5.6 minutes on the IBM 7094.

Although no numerical results are presented for a shell of revolution under asymmetric loading, it is postulated that DRASTIC will give as accurate a set of results for this type of problem as for axisymmetric response. The reasons are as follows: the accuracy of the stiffness matrix, $\mathbf{K}^i$, has been well checked out (References 5 and 6); the mass matrix, $\mathbf{M}^i$, has the same coefficients for all harmonics; and the solution of the equations of motion (Equation 1) is performed one harmonic at a time, as accurately for the i^{th} harmonic ($i \neq 0$) as for the zeroth harmonic.

DISCUSSION

The finite element - matrix displacement approach to the dynamic analysis of shells of revolution has been presented with the intention of providing a detailed examination into the development of the method. This is necessary background information for use of the technique and associated computer code in its present form. Such use permits solution of a wide variety of complex shell structure problems, not only for axisymmetric deformation but for asymmetric response. Focusing on the latter, the dynamic response of axisymmetric shells with arbitrary meridional shape, arbitrary displacement restraints, and varying material properties and thickness in the meridional direction, under arbitrary asymmetric force distributions is presented. Although a shell analysis of this complexity is in itself a powerful tool for the structural engineer, the method has importance for future applications. With the analysis divided into the representation of the mass and stiffness of the structure and mathematical solution of the equations of motion, it is seen that extensions to more complex structural problems required only modification of the stiffness and mass matrix. The dynamic solution presented above will be just as valid. For example, anisotropic multilayer shells may be analyzed with the same facility as isotropic single layer shells are now handled.

REFERENCES

1. Klein, S., Matrix Analysis of Shell Structures, S. M. Thesis, ASRL-TR-121-12, Department of Aeronautics and Astronautics, MIT, Cambridge, Mass., June, 1964.

2. Percy, J. H., Pian, T. H. H., Klein, S., and Navaratna, D. R., Application of Matrix Displacement Method to the Linear Elastic Analysis of Shells of Revolution, AIAA Paper No. 65-142, presented at the AIAA 2nd Aerospace Sciences Meeting, New York, 25-27 January, 1965.

3. Percy, J. H., Pian, T. H. H., Navaratna, D. R., and Klein, S., Application of the Matrix Displacement Method to the Linear Elastic Analysis of Shells of Revolution, ASRL-TR-121-7, Aeroelastic and Structures Research Laboratory, MIT, Cambridge, Mass, January 1965.

4. Percy, J. H., Navaratna, D. R., and Klein, S., SABOR I: A FORTRAN Program for the Linear Elastic Analysis of Thin Shells of Revolution under Axisymmetric Loading by Using the Matrix Displacement Method, TR-121-5, Aeroelastic and Structures Research Laboratory, MIT, Cambridge, Mass., April 1965.

5. Percy, J. H., Navaratna, D. R., and Klein, S., SABOR III: A FORTRAN Program for the Linear Elastic Analysis of Thin Shells of Revolution under Asymmetric or Axisymmetric Loading by Using the Matrix Displacement Method, TR-121-6, Aeroelastic and Structures Research Laboratory, MIT, Cambridge, Mass., May 1965.

6. Klein, S., A Study of the Matrix Displacement Method as Applied to Shells of Revolution. Paper presented at the Conference on Matrix Methods in Structural Mechanics, Wright-Patterson Air Force Base, Ohio, 26-28 October 1965.

7. Archer, J. S., "Consistent Mass Matrix for Distributed Mass Systems" (Proceedings of the American Society of Civil Engineers) ASCE Structural Division Journal, Vol. 89, Part I, No. ST 4, pp. 161-178, August 1963.

8. Chan, S. P., Cox, H. L., and Benfield, W. A., "Transient Analysis of Forced Vibrations of Complex Structural-Mechanical Systems," Journal of the Royal Aeronautical Society, Vol. 66, pp. 457-460, July 1962.

9. Salvadori, M. G., Baron, M. L., Numerical Methods of Engineering, pp. 27-32, Prentice-Hall, Inc., N.J. 1961.

10. Koval, L. R., and Bhuta, P. G., Dynamic Response of Shallow Spherical Shells, EM 13-21, TRW Space Technology Laboratories, October 1963.

APPENDIX

LIST OF MATRICES

In this appendix are listed two matrices referred to in the text of the paper.

V Matrix (see Equation 10).

$$\begin{bmatrix} r & rs & rs^2 & rs^3 & 0 & 0 & 0 & 0 \\ rs & rs^2 & rs^3 & rs^4 & 0 & 0 & 0 & 0 \\ rs^2 & rs^3 & rs^4 & rs^5 & 0 & 0 & 0 & 0 \\ rs^3 & rs^4 & rs^5 & rs^6 & 0 & 0 & 0 & 0 \\ 0 & 0 & 0 & 0 & r & rs & 0 & 0 \\ 0 & 0 & 0 & 0 & rs & rs^2 & 0 & 0 \\ 0 & 0 & 0 & 0 & 0 & 0 & r & rs \\ 0 & 0 & 0 & 0 & 0 & 0 & rs & rs^2 \end{bmatrix}$$

P Matrix (see Equation 11).

The nonzero elements of the **P** matrix are:

$$P_{11} = P_{55} = P_{77} = A_{1,0}$$

$$P_{12} = P_{21} = P_{56} = P_{65} = P_{78} = P_{87} = A_{1,1}$$

$$P_{22} = P_{13} = P_{31} = P_{66} = P_{88} = A_{1,2}$$

$$P_{14} = P_{41} = P_{23} = P_{32} = A_{1,3}$$

$$P_{33} = P_{24} = P_{42} = A_{1,4}$$

$$P_{34} = P_{43} = A_{1,5}$$

$$P_{44} = A_{1,6}$$

where

$$A_{\alpha,\beta} = \int_0^{\ell} r^{\alpha} s^{\beta} \, ds$$

ADDENDUM

E. P. Popov* and H. Y. Chow**
University of California
Berkeley, California

The paper by S. Klein and R. J. Sylvester presents important information for practical analysis of shells of revolution. The chosen approach based on the matrix displacement method of analysis is well founded (References, 1, 2). Likewise, finite elements in the form of conical frusta joined at nodal circles have been found to be effective in the solution of static problems. The extension of the procedure to dynamic problems to the level of rapidly solving actual problems is a significant accomplishment. The writers have also extended some of their earlier work (References, 3, 4) to include axisymmetrical response of shells of revolution to dynamic loads. An outline of the developed solution***, which in several respects differs from the one by S. Klein and R. J. Sylvester followed by two examples is given herein. The data for one of the examples are taken from the preceding paper. Excellent agreement between the two solutions is found which serves to corroborate the results found independently. In the other example a circular plate with a ring load is analysed using the exact element stiffness matrix and the element mass matrix based on exact static edge-loading displacements. The same results are found with two as well as with 20 finite elements. For complex systems this fact may be of importance.

---

* Professor of Civil Engineering
** Graduate Student
*** A more complete report by the writers to NASA is in preparation.

EQUATIONS OF MOTION

Any shell of revolution can be approximated with a sufficient degree of accuracy for practical purposes by a finite number of elements consisting of plate, conical, or cylindrical rings. All of such elements are joined at nodal circles. The matrix formulation of the general dynamic response of such a substitute structure can be stated as follows:

$$\mathbf{M}\,\ddot{\mathbf{q}}(t) + \mathbf{K}\,\mathbf{q}(t) = \mathbf{f}(t) \tag{1}$$

where the column matrices $\mathbf{f}(t)$ and $\mathbf{q}(t)$ are, respectively, the generalized forces and generalized displacements of the structure. The mass matrix $\mathbf{M}$ and the structural stiffness matrix $\mathbf{K}$ are symmetrical and furthermore $\mathbf{K}$ is a positive definite. Therefore, Equation 1 can be uncoupled (Reference 5) and solved using the normal mode superposition technique.

A direct numerical integration method was used in this investigation to solve the uncoupled second order differential equations. For each mode a different interval of time for each integral is used. This procedure retains the necessary accuracy for the higher frequency modes and avoids the unnecessary, time consuming computations for the lower frequencies.

The mass matrix $\mathbf{M}$ and the stiffness matrix $\mathbf{K}$ for a whole structure are determined from the assemblage of basic solutions for the elements. Since this procedure is well known, only the formulation used to establish element stiffness and mass matrices is discussed here.

THE ELEMENT STIFFNESS AND MASS MATRICES

The homogeneous solution for a basic finite element can be expressed in matrix form as follows:

$$\mathbf{d}_i\ (s,t) = \begin{bmatrix} X(s,t) \\ V(s,t) \\ W(s,t) \end{bmatrix} = \mathbf{X}_{ij}\ (s)\ \ \mathbf{A}_j\ (t) \tag{2}$$

and

$$\mathbf{S}_i\ (s,t) = \begin{bmatrix} M_s(s,t) \\ N_s(s,t) \\ Q_s(s,t) \end{bmatrix} = \mathbf{Y}_{ij}\ (s)\ \ \mathbf{A}_j(t) \tag{3}$$

and

$$i = 1, 2, 3 \text{ and } j = 1, 2 \ldots\ldots, 6$$

where $\mathbf{d}_i$ (s, t) are displacement-variables which are comprised of rotational X(s, t), meridional V(s, t), and normal W(s, t) displacements; $\mathbf{S}_i$ (s, t) are force-variables which consist of meridional moments M_s(s, t), meridional stress-resultants N_s(s, t), and shearing stress-resultants Q_s(s, t).

$\mathbf{X}_{ij}$ (s) and $\mathbf{Y}_{ij}$ (s) are two (3 x 6) matrices which are obtained from the general solutions of a static edge-loading problem for a basic element. $\mathbf{A}_j$ (t) is a column matrix which can be determined from the nodal displacements at each end of the shell segment.

Closed form solutions of Equation 1 were developed (References 3 and 4 and authors report to NASA in preparation) for circular annular rings, conical frusta, and cylindrical segments. In this formulation, if such elements represent portions of the actual structure, no limitation on the size of elements needs to be placed. Only the total number of elements may become a problem.

Using closed form solutions of Equation 1, the element stiffness matrices $\mathbf{k}$ were developed and programmed for the above type of elements. The basic relation for determining $\mathbf{k}$ can be deduced by considering strain energy U of an element, and can be shown to be

$$\mathbf{k} = \mathbf{T}^T \ \mathbf{C} \ \mathbf{B}^{-1} \ \mathbf{T} \tag{4}$$

where $\mathbf{T}$ is a coordinate transformation matrix relating shell element coordinates to the system coordinates, and matrices $\mathbf{C}$ and $\mathbf{B}$ are matrices $\mathbf{Y}$ and $\mathbf{X}$, respectively, upon substitution into them of the two boundary values of s. Since this relationship in but a slightly different form was previously reported (References 3 and 4), no further comments will be made here.

To determine the mass matrix $\mathbf{m}$ for an element, the fundametal displacement-variable vector $\mathbf{d}_i$, Equation 2, must be re-cast in terms of its six generalized system (global) coordinates, i.e.,

$$\mathbf{d}_i (s,t) = \mathbf{X}_{ij}(s) \ \mathbf{B}_{jk}^{-1} \ \mathbf{T}_{km} \ \mathbf{q}_m (t) \tag{5}$$

here i = 1, 2, 3 and j, k, m, = 1, 2, 3....6.

and $\mathbf{q}_m$ (t) represents six nodal displacements of an element in system coordinates.

The general expression for the kinetic energy T(t) (References 6 and 7) of a shell element can be written as

$$T(t) = \frac{1}{2} \int_s \left[m \ \rho_A^2 \ \dot{X}^2 (s,t) + m \ \dot{V}^2 (s,t) + m \ \dot{W}^2 (s,t) \right] 2\pi \ r(s) \ ds \tag{6}$$

where m is mass per unit of surface area, and ρ_A is the radius of gyration of the section of a shell segment.

Upon substituting the displacement variables involved in Equation 5 into Equation 6, one obtains

$$T(t) = \frac{1}{2} (\dot{\mathbf{q}}(t))^T \ \mathbf{T}^T (\mathbf{B}^{-1})^T \int_s 2\pi \ \mathbf{E}(s) \ r(s) \ ds \ \mathbf{B}^{-1} \ \mathbf{T} \ \dot{\mathbf{q}}(t) \tag{7}$$

By comparing this complex matrix expression with the usual one for kinetic energy, definition of the mass matrix $\mathbf{m}$ is obtained:

$$\mathbf{m} = \mathbf{T}^T (\mathbf{B}^{-1})^T \int_s 2\pi \ \mathbf{E}(s) \ r(s) \ ds \ \mathbf{B}^{-1} \ \mathbf{T} \tag{8}$$

This element mass matrix $\mathbf{m}$ was determined and programmed for annular rings using an exact displacement field. For conical frusta the mass matrix $\mathbf{m}$ for an element was developed on the basis of an assumed polynomial function to represent the displacement field. For the above reason, the range of applicability of the developed program as it relates to the size of elements is different for the two cases.

EXAMPLES AND CONCLUSIONS

As the first example consider an elastic circular plate clamped along the edge subjected to a ring load as shown in Figure A-1. The ring load P is applied as a step function in time. To determine the dynamic response of this plate by the developed method, only two elements* need to be used, since both the **m** and **k** matrices are programmed using the exact displacement field. Alternatively, an arbitrary number of elements may be used and 20 elements were selected to obtain a solution for comparative purposes. The results of the two solutions are plotted in Figures A-4a and A-4b. Differences between the two solutions are negligible. The solution based on the use of 20 elements actually is a little less accurate due to the unavoidable accumulation of numerical errors.

The second example is for the dynamic response of a shallow spherical cap shown in Figure A-2. The data are from the Klein and Sylvester example. The results of an output for a 14-element solution are shown in Figures A-5a, A-5b and A-5c. These results are seen to be in excellent agreement with the Klein and Sylvester solution and this provides a good check on the two independently developed programs.

The developed program of course also can be successfully applied to deep shells as well as to shell-like enclosures. For example, the dynamic response of the sphere shown in Figure A-3 was readily found using a solution based on 50 elements. (Results not reported here).

The dynamic response of linear elastic shells of revolution of arbitrary meridian shape and thickness variation can be determined using the finite element approach. The accuracy appears to be excellent, and once a program is developed a solution is achieved very rapidly. Occasionally, solutions based on exact displacement fields for element mass and stiffness matrices may prove advantageous.

ACKNOWLEDGEMENTS

The authors wish to acknowledge with gratitude the financial support of NASA which made possible the development of the reported programs.

REFERENCES

1. Argyrus, J. H., Kelsey, S., "Energy Theorems and Structural Analysis", Butterworth and Co., 1960.

2. Turner, M. J., Clough, R. J., Martin, H. C. and Topp, L. J., "Stiffness and Deflection Analysis of Complex Structures". Journal Aero. Society, 23, Sept., 1956.

3. Lu, Z. A., Penzien, J., Popov, E. P., "Finite Element Solution for Thin Shells of Revolution", IER, SESM 63-3, University of California, Berkeley, California, September 1963, also re-issued as NASA Report CR-37, Washington, D. C., July 1964.

4. Popov, E. P., Penzien, J. Lu, Z. A., "Finite Element Solution for Axisymmetrical Shells", Proceedings of the American Society of Civil Engineers, Journal of the Engineering Mechanics Division, Vol. 90, EMS, October 1964, pp. 119-145.

5. Friedman, B., "Principles and Techniques of Applied Mathematics", John Wiley and Sons, Inc., 1960.

* A disk of 10 in. radius, and an annular ring bounded by 10 in. and 20 in. radii.

6. Archer, J. S., "Consistent Mass Matrix for Distributed Mass System", Proceedings of the American Society of Civil Engineer Journal of the Structural Division, 89 No. ST 4, pp. 161-178, August, 1963, Part I.

7. Bisplinghoff, R. L., Ashley, H., Halfman, R. L., "Aeroelasticity", Addison-Wesley Publishing Company, Inc., 1955.

CLOSURE

Stanley Klein*
Aerospace Corporation
San Bernardino, California

The author wishes to thank E. P. Popov and H. Y. Chow for their contribution in the form of an addendum to the paper presented herein. Just as using a stiffness matrix derived from an exact solution of a conical frustum under edge loads provided a measure of the excellent accuracy obtained using the matrix displacement method, E. P. Popov and his colleagues have now provided a firm foundation and independent check of the direct numerical integration of the coupled 2nd order shell equations presented in this paper.

It must be pointed out that the use of the standard normal mode superposition technique used by E. P. Popov and H. Y. Chow was considered by the author and his colleagues. In fact, a computer program, FAMOUS (Reference 1), was written to obtain the natural modes and frequencies for a shell structure represented by 100-160 degrees of freedom (40-50 finite elements). Results obtained with this code indicated that it would be difficult to obtain many of the higher frequencies with a good degree of accuracy. Since high frequency response is of interest in these problems coupled with the fact that the present SABOR and DRASTIC codes handle much larger problems than discussed here (i. e., 125-200 finite elements or 500-800 degrees of freedom), it became necessary to abandon the normal mode approach.

It must also be considered that using the normal mode approach even for relatively small problems (less than 100 D.O.F.), it becomes necessary to obtain a set of natural frequencies, make a decision as to which ones are important, solve the uncoupled 2nd order differential equations for each frequency after finding an appropriate time step for each solution, and then finally superpose the individual results. This can mean a large amount of computation and engineering time. The direct solution of the coupled 2nd order equations yields a further advantage in that it provides a good stepping stone towards solving the dynamic nonlinear shell response problem using a stepwise linear incremental approach.

An item of future importance that requires mentioning is the very interesting observation made by E. P. Popov, H. Y. Chow and the author that increasing the number of finite elements does not increase the accuracy of the results in the dynamic case as it does in the static case. This is only a preliminary observation but its effect on future work in this area requires that it be carefully investigated.

Since the writing of the preceding paper, some very interesting observations have been made which bear heavily on the calculation of stress resultants, both statically and dynamically. It has been found that the use of local element stiffness matrices to calculate stresses at the edges of each element produces large errors in membrane regions of shells. Methods to eliminate these errors, such as correcting for the effect of the approximate distribution of surface loads applied as line loads at the nodes, or calculating stresses directly from the

* Member of the Technical Staff

stress-displacement relations using either a differentiation of the assumed displacements or a finite difference representation of the derivatives, have been checked out. A detailed comparison of these methods will be published shortly (Reference 2). These techniques have reduced the problem of residual moments, under much discussion, to negligible proportions, and with the introduction of curved finite elements, the residual moments will be virtually nonexistent.

In closing, the author wishes to express his gratitude to the chairman and all concerned with the conference for providing an excellent forum for discussing the progress being made in this special area of structural mechanics.

REFERENCES

1.) Young, R. and McCallum H., The Determination of Frequencies and Modes of Undamped Structures Using the Finite-Element Stiffness and Consistent-Mass Matrices, Massachusetts Institute of Technology, Aeroelastic and Structures Research Laboratory, ASRL TR 121-8, June, 1965.

2.) Navaratna, D. R., private communication, 1965.

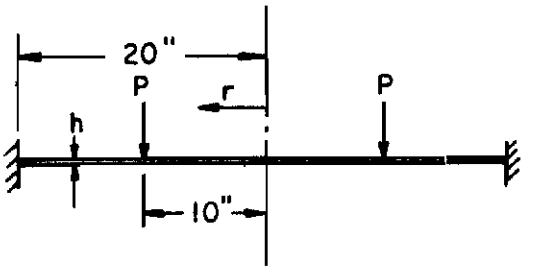

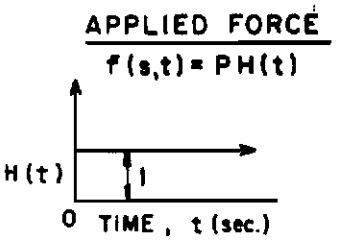

h = 1.0 IN. $E = 10 \times 10^7$ LB./IN.^{2}

$\nu = 0.3$ $\rho = 0.10$ LB./IN.^{3}

P = 159.15 LB./IN.

Figure A-1. A Circular Plate Under Dynamic Loading

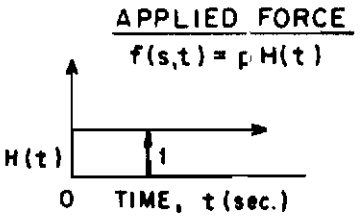

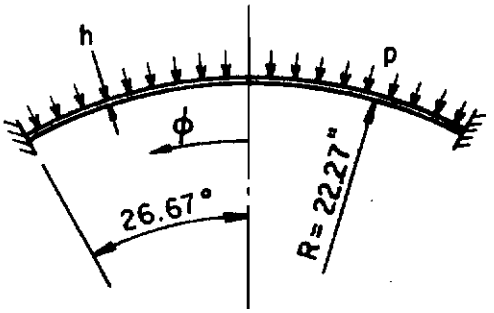

h = 0.41 IN. $E = 10.5 \times 10^7$ LB./IN.^{2}

$\nu = 0.3$ $\rho = 0.09506$ LB./IN.^{3}

p = 100 LB./IN.^{2}

Figure A-2. A Spherical Cap Under Dynamic Loading

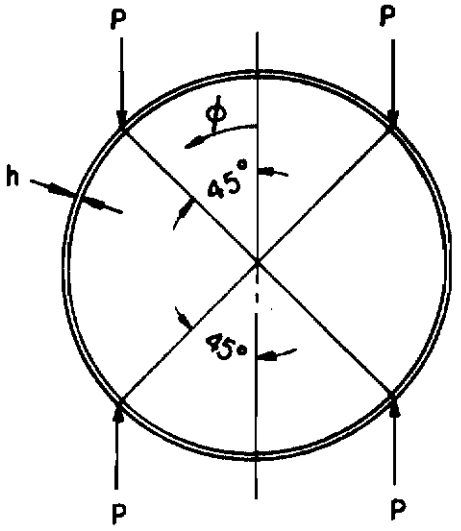

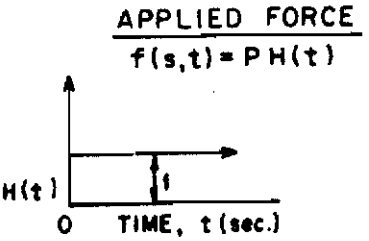

h = 0.41 IN. $E = 10.5 \times 10^7$ LB./IN.^{2}

$\nu = 0.3$ $\rho = 0.10$ LB./IN.^{3}

P = 1010.7 LB./IN.

Figure A-3. A Sphere Under Dynamic Loading

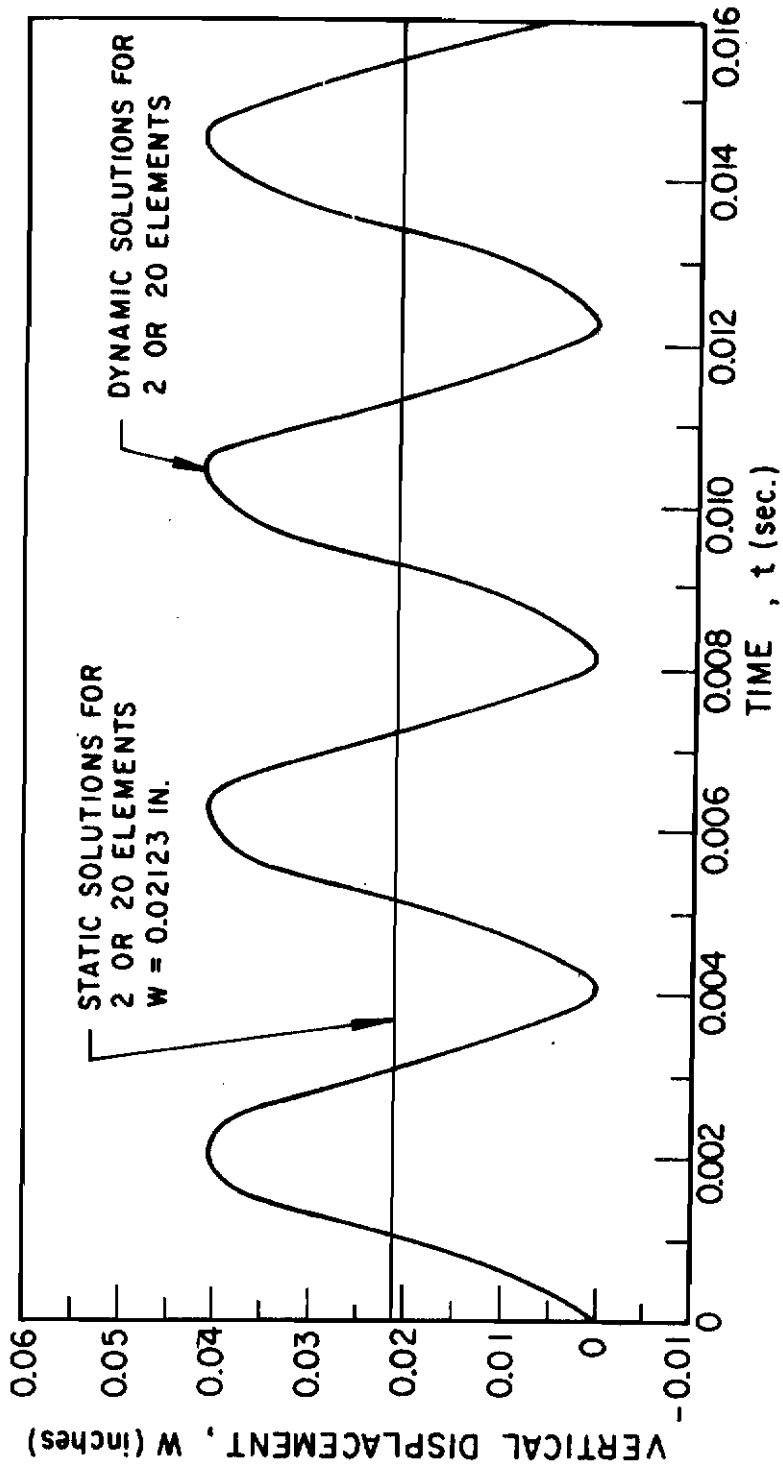

Figure A-4a. Vertical Displacement Response at r = 10 In. for the Circular Plate

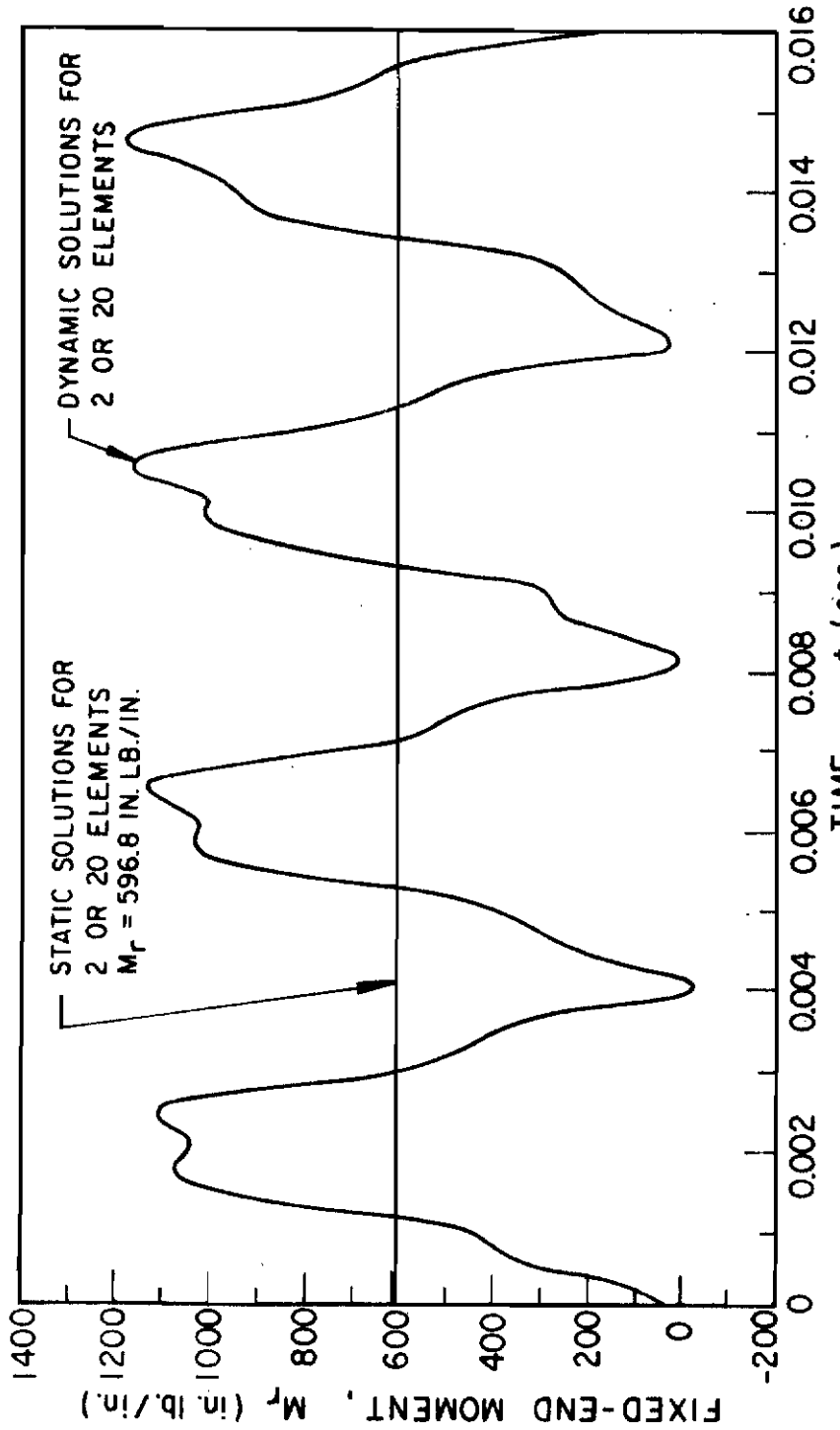

Figure A-4b. Fixed-End Moment Response at r = 20 In. for the Circular Plate

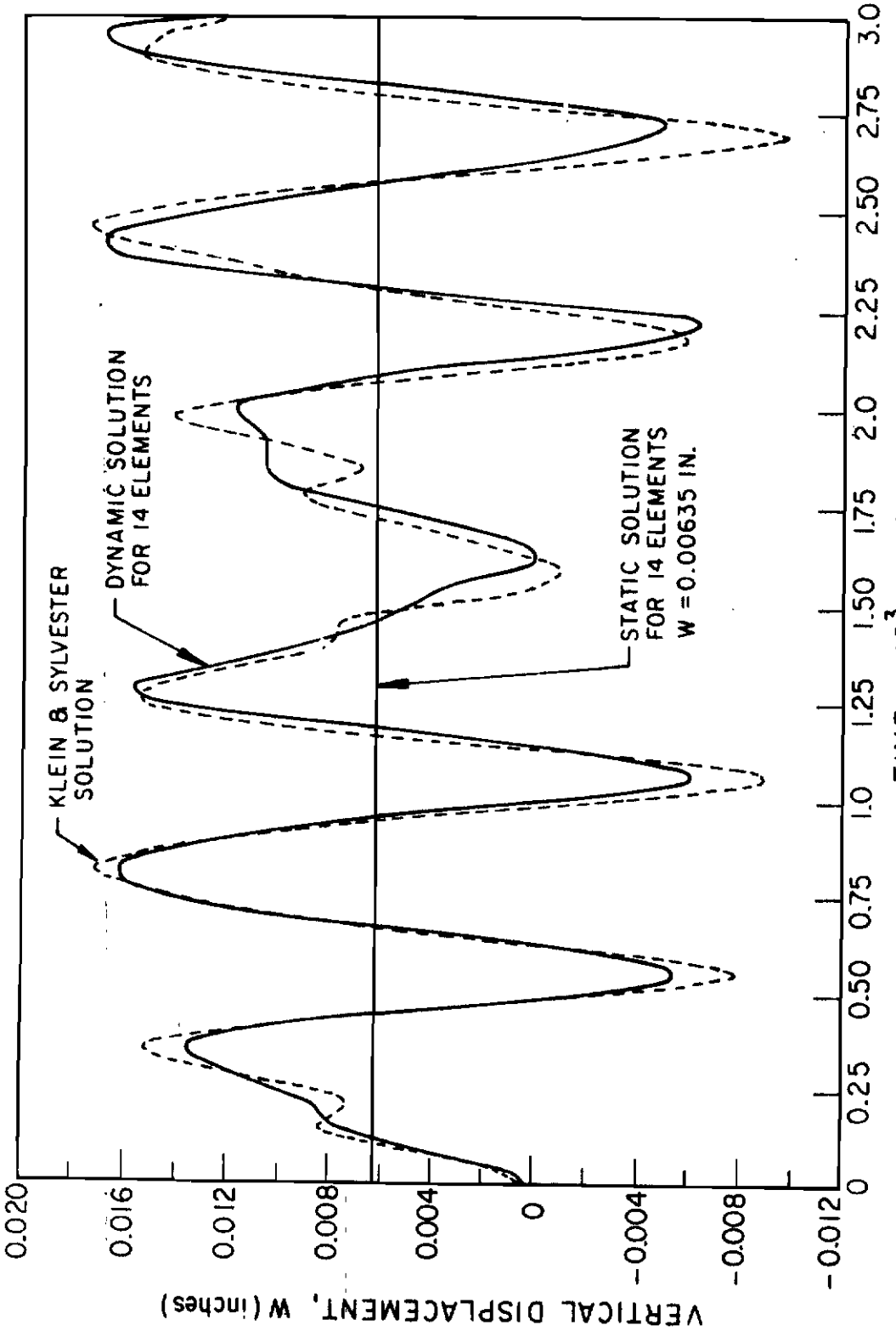

Figure A-5a. Vertical Displacement Response at $\phi = 0°$ for the Spherical Cap

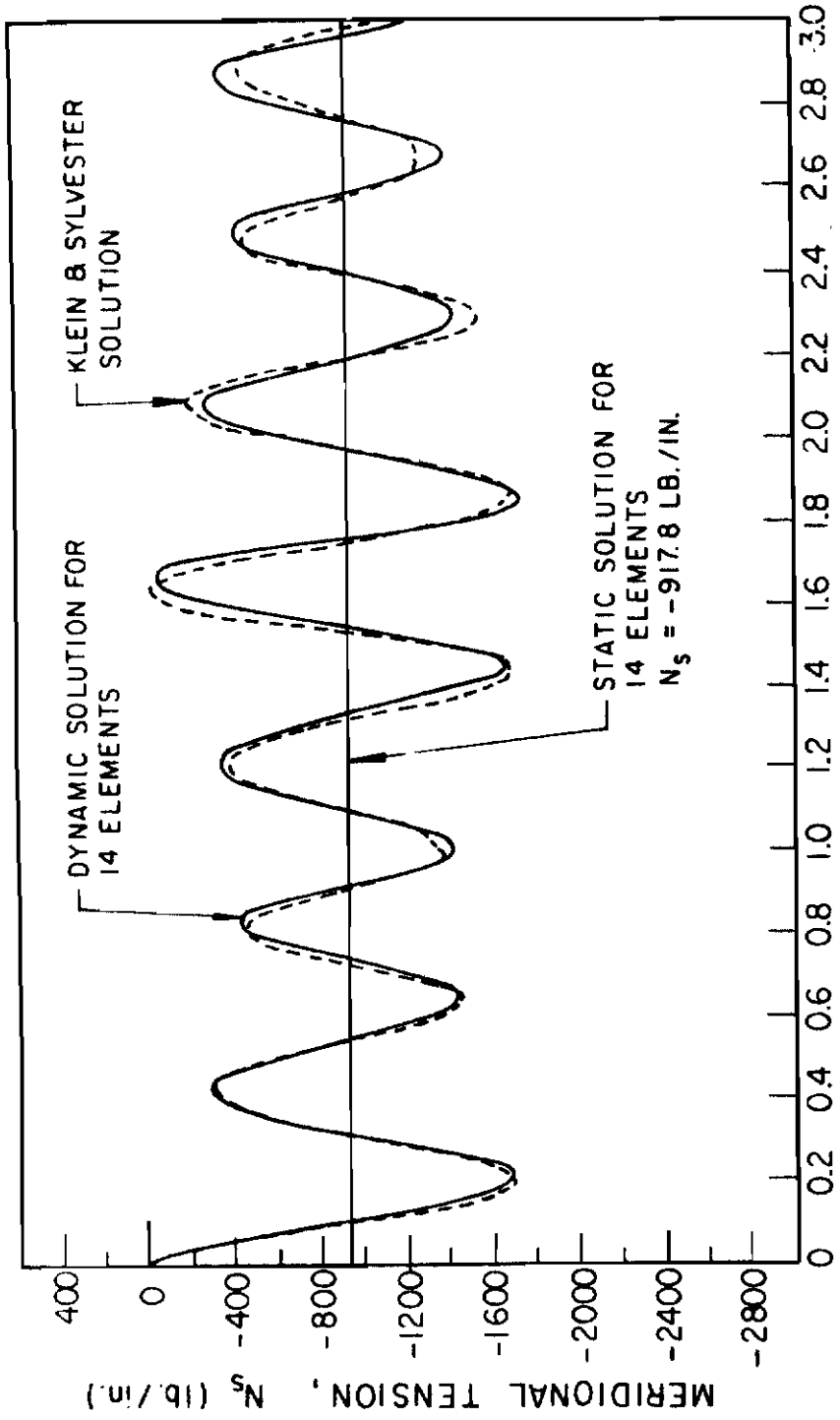

Figure A-5b. Meridional Tension Response at ϕ= 26.67° for the Spherical Cap

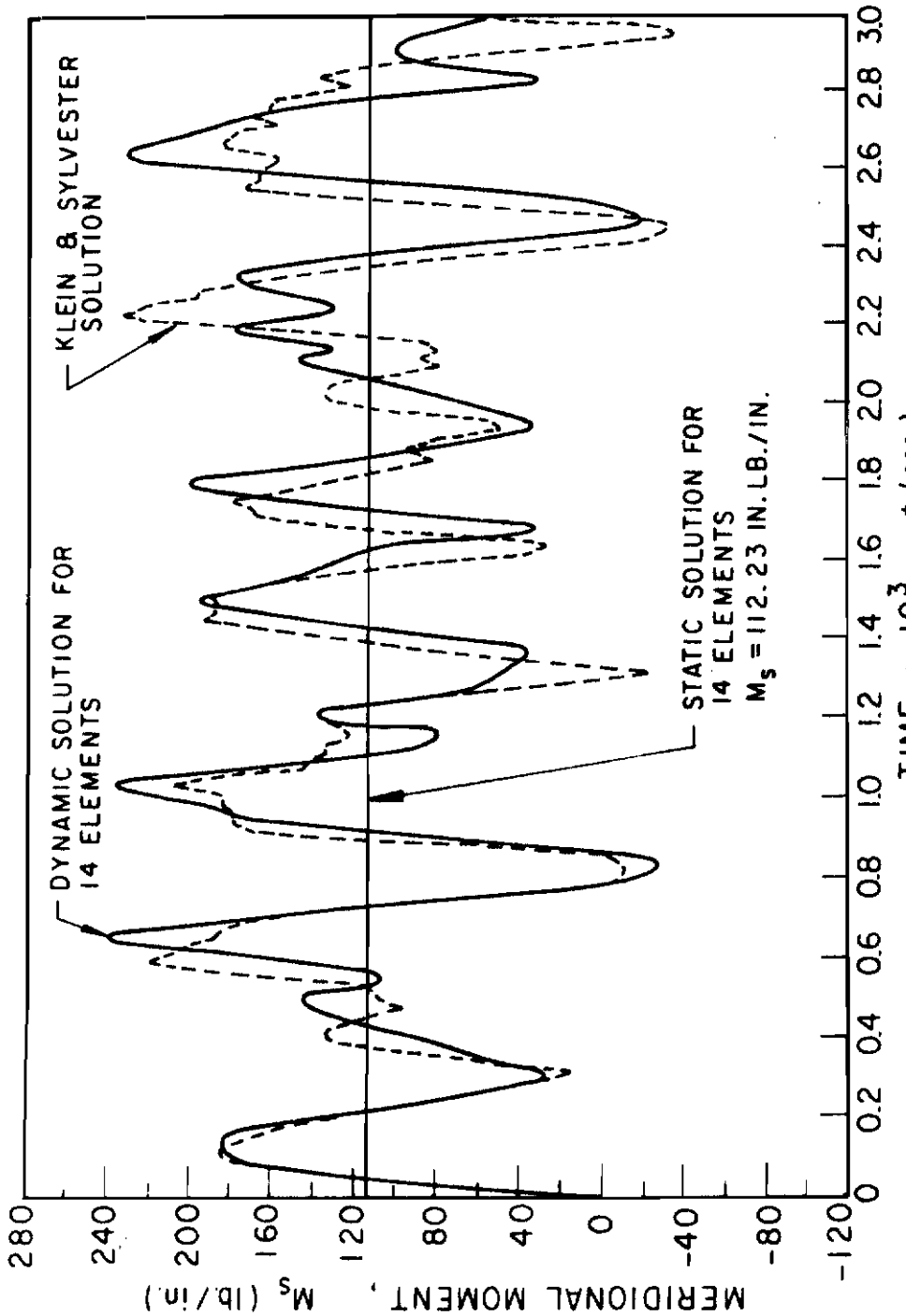

Figure A-5c. Meridional Moment Response at ϕ = 26.67° for the Spherical Cap